ChemPubSoc Europe
DOI: 10.1002/ejic.201700875
EurJIC European Journal of Inorganic Chemistry
Full Paper

Cobalt Oxidation Catalysts

A Bis(μ-chlorido)-Bridged Cobalt(II) Complex with Silyl-Containing Schiff Base as a Catalyst Precursor in the Solvent-Free Oxidation of Cyclohexane

Mirela-Fernanda Zaltariov,[a] Veacheslav Vieru,[b] Michal Zalibera,[c] Maria Cazacu,[a] Nuno M. R. Martins,[d] Luísa M. D. R. S. Martins*[d,e] Peter Rapta,[c] Ghenadie Novitchi,[f] Sergiu Shova,[a] Armando J. L. Pombeiro,[d] and Vladimir B. Arion*[g]

Abstract: A new bis(μ-chlorido)-bridged cobalt(II) complex $[Co_2(\mu\text{-}Cl)_2(HL^2)_4][CoCl_4]$ (**1**), where HL^2 is a silyl-containing Schiff base, was synthesised. The structure of this compound was established by X-ray crystallography revealing a zwitterionic form adopted by the organic ligand. The temperature dependence of the magnetic susceptibility and the field dependence of the magnetisation indicate the presence of ferromagnetic interactions between paramagnetic d^7 cobalt(II) centres (S_{Co} = 3/2). The exchange coupling parameter $J(Co1–Co2)$ = +7.0 cm^{-1} extracted from broken-symmetry (BS) DFT calculations agrees well with the value of +8.8 cm^{-1} determined from the experimental data by fitting them with the Hamiltonian $\hat{H} = -J^{\mathrm{exch}}_{\mathrm{Co1-Co2}}\hat{\mathbf{S}}_{\mathrm{Co1}}\cdot\hat{\mathbf{S}}_{\mathrm{Co2}}$. Electrochemical studies indicate that complex **1** is inefficient as a catalyst in electrochemical reduction of protons. One of the reasons is the low stability of the complex in solution. In contrast, **1** acts as an effective homogeneous (pre)catalyst in the microwave-assisted neat oxidation of cyclohexane with aqueous *t*BuOOH (TBHP). The possible mechanism of catalytic oxidation and other advantages of using **1** in the oxidation of cycloalkanes are discussed.

Introduction

The design and synthesis of earth-abundant metal complexes as efficient catalysts for water splitting by reduction or oxidation reactions with low overpotentials and good stability remains a significant challenge.[1,2] During the last few years cobalt complexes have received particular attention.[3–8]

Dinuclear μ-chlorido-bridged cobalt(III) complexes supported by tetradentate ligands of the type $L_2Co_2Cl_2$ were also reported to catalyse the electrolytic and photolytic reduction of water.[9–11] In particular, the dicobalt(III) complex with 2-pyridylamino-*N*,*N*-bis(2-methylene-4,6-dimethyl)phenol was found to catalyse water reduction to hydrogen with a TOF of 922 mol of H_2 per mol of catalyst per hour at pH 7.0, while at pH 4 in the presence of $[Ru(bpy)_3]Cl_2$ and ascorbic acid when irradiated with blue light hydrogen was produced with a TON of 14460 mol of H_2 per mol of catalyst.[11] Photoinduced oxygen evolution was reported for a dinuclear μ-peroxido-μ-hydroxido-bridged polypyridine complex $[(TPA)Co(\mu\text{-}OH)(\mu\text{-}O_2)Co(TPA)](ClO_4)_3$ [TPA = tris(2-pyridylmethyl)amine] or double-helical dicobalt(II) complex $[Co_2(spy)_2](ClO_4)_4$ (spy = 2,2′:6′,2′′:6′′,2′′′:6′′′,2′′′′:6′′′′,2′′′′′-sexipyridine) in the presence of $[Ru(bpy)_3]Cl_2$ and $S_2O_8{}^{2-}$.[12,13]

In addition, the interest in the synthesis of cobalt complexes is fuelled by their ability to act as catalysts or catalyst precursors in oxidation reactions including those of academic and industrial relevance. Robust cobalt(III) sepulchrate (sep) complexes $[Co(sep)]Cl_3$ and $[Co(sep)]_2(SO_4)_3$ act as homogeneous catalysts in the oxidation of styrene with benzaldehyde as the main product.[14] The cobalt(III) complex $[Co_2(amp)_2(\mu\text{-}imp)_2Cl_2]Cl_2\cdot 2H_2O$, where amp = 2-aminomethylpyridine and imp = 2-iminomethylpyridine anion, was reported as a functional model for phenoxazinone synthase.[15] The compound promotes the oxidative coupling of 2-aminophenol to the 2-aminophenoxazinone chromophore in methanol saturated with O_2. A mononuclear macrocyclic picolinamide complex catalyses efficiently

---

[a] Inorganic Polymers Department, “Petru Poni” Institute of Macromolecular Chemistry,
Aleea Gr. Ghica Voda 41 A, Iasi 700487, Romania
[b] Theory of Nanomaterials Group, Katholieke Universiteit Leuven,
Celestijnenlaan 200F, 3001 Heverlee, Belgium
[c] Institute of Physical Chemistry and Chemical Physics, Slovak University of Technology,
Radlinského 9, 81237 Bratislava, Slovak Republic
[d] Centro de Química Estrutural, Instituto Superior Técnico, Universidade de Lisboa,
Av. Rovisco Pais, 1049-001 Lisboa, Portugal
[e] Chemical Engineering Department, Instituto Superior de Engenharia de Lisboa, Instituto Politécnico de Lisboa,
Rua Conselheiro Emídio Navarro, 1059-007 Lisboa, Portugal
E-mail: lmartins@deq.isel.ipl.pt
luisamargaridamartins.weebly.com
[f] Laboratoire National des Champs Magnétiques Intenses, UPR CNRS 3228,
25 rue des Martyrs, B. P. 166, 38042 Grenoble Cedex 9, France
[g] University of Vienna, Faculty of Chemistry, Institute of Inorganic Chemistry,
Währinger Strasse 42, 1090 Vienna, Austria
E-mail: vladimir.arion@univie.ac.at
anorg-chemie.univie.ac.at/magniolaPublic/Research/Bioinorganic-chemistry/Group-V-Arion.html

Supporting information and ORCID(s) from the author(s) for this article are available on the WWW under https://doi.org/10.1002/ejic.201700875.

the conversion of cyclohexene into 2-cyclohexen-1-one,[16] while a dinuclear cobalt(II) complex $[CoCl(\mu\text{-}Cl)(HpzPh)_3]_2$ (Hpz^{Ph} = 3-phenylpyrazole) acts as catalyst precursor in the peroxidative oxidation of cyclohexane to cyclohexanol and cyclohexanone under mild conditions.[17] The dinuclear complex permitted to achieve overall TONs up to 223 mol of product per mol of catalyst. This value was markedly higher than that determined for the related mononuclear cobalt(II) complex $[CoCl_2(Hpz^{Ph})_4]$ with a total TON of 105 (although similar if calculated per Co atom) or the TONs reported for copper and vanadium complexes.[18–20]

Being interested in metal complexes with ligands based on both silane and siloxane (either open-chain or macrocyclic) we reported recently on metal complexes with Schiff bases resulting from reactions of 1,3-bis(3-aminopropyl)tetramethyldisiloxane with substituted 2-hydroxybenzaldehydes,[21,22] pyrrole-2-carbaldehyde[23] and 2,6-diformyl-4-methylphenol (DFF)[24,25] or trimethylsilylmethyl *p*-aminobenzoate with DFF.[25] The tetranuclear copper(II) complexes $[Cu_4(\mu_4\text{-}O)(L^1)Cl_4]$ and $[Cu_4(\mu_4\text{-}O)(L^2)_2Cl_4]$, where H_2L^1 is a macrocyclic ligand resulting from [2+2] condensation of 1,3-bis(3-aminopropyl)tetramethyldisiloxane and DFF and HL^2 is a 1:2 condensation product of trimethylsilylmethyl *p*-aminobenzoate and DFF, are effective catalyst precursors for hydrocarboxylation of a series of linear and cyclic alkanes. Yields up to 36 % were obtained based on the alkane and peroxidative oxidation of cyclohexane to cyclohexanol and cyclohexanone.[25]

Herein we report on the synthesis of a dinuclear bis(μ-chlorido)-bridged cobalt(II) complex $[Co_2(HL^2)_4(\mu\text{-}Cl)_2][CoCl_4]$ (**1**), its magnetic properties and electrochemical behaviour, as well as catalytic activity in the microwave-assisted solvent-free oxidation of cyclohexane to cyclohexanol and cyclohexanone.

Results and Discussion

Synthesis

By reaction of 2,6-diformyl-4-methylphenol with trimethylsilylmethyl *p*-aminobenzoate in a 1:2 molar ratio in a methanol/chloroform (1:1) mixture the Schiff base HL^2 (Scheme 1) was generated in situ. The formation of the latter was previously confirmed by spectroscopic and analytical data.[25] Further addition of $CoCl_2{\cdot}6H_2O$ and a few drops of triethylamine as a base afforded a crude product, which after recrystallization from chloroform/acetonitrile (1:1) was isolated as crystalline material **1** of X-ray diffraction quality. The result of single-crystal X-ray crystallography (see below) was also in accord with the elemental analysis of a bulk sample. The IR spectrum reveals the presence of the characteristic bands assigned to the azomethine group at 1622 cm^{-1}, the symmetric and asymmetric deformation vibrations of the methyl groups attached to silicon atoms at 1249 and 1414 cm^{-1}, respectively, the methyl rocking and the Si–C stretching vibrations at 854 cm^{-1} (Figure S1). Strong bands at 1714 and 1110 cm^{-1} are attributed to the C=O and C–O stretching vibrations of the ester group, respectively, while weak bands in the spectral region of 395–519 cm^{-1} are associated with the new Co–N and Co–O coordination bonds, not present in the proligand.[25]

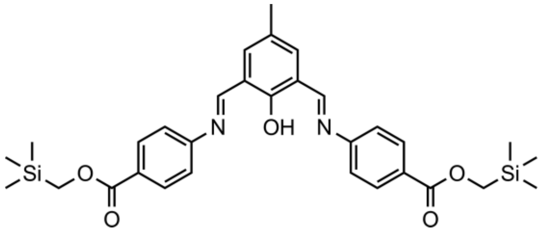

Scheme 1. Line drawing of the Schiff base HL^2.

In the mass spectrum of **1** in acetonitrile measured in positive ion mode a doubly charged peak at *m/z* = 1272.3258 is observed, which was assigned to $[Co_3Cl_2(L)_2(HL)_2]^{2+}$ {calcd. for $[Co_3Cl_2(C_{31}H_{37}N_2O_5Si_2)_2(C_{31}H_{38}N_2O_5Si_2)_2]^{2+}$ 1272.3253}. A comparison of the measured and calculated isotopic patterns is shown in Figure S2. The UV/Vis spectrum of **1** in acetonitrile shows strong absorption bands at 262 and 314 nm assigned to π–π* transitions involving the benzene ring and imine (CH=N) chromophore, a ligand-to-metal charge-transfer (LMCT) band at 470 nm and four weak absorptions with maxima at 585, 631, 660 and 685 nm due to d–d transitions (Figure S3).

Crystal Structure

According to X-ray diffraction study the crystal structure of **1** consists of $[Co_2Cl_2(HL^2)_4]^{2+}$ dinuclear cations, $[CoCl_4]^{2-}$ counteranions and cocrystallised acetonitrile molecules, so that the final composition as well as the charge balance correspond to the formula $[Co_2Cl_2(HL^2)_4][CoCl_4]{\cdot}4.5CH_3CN$. As shown in Figure 1, the dicationic unit is formed by four HL^2 ligands, two cobalt ions and two Cl^- ions. The observed Co–N and Co–O bond lengths (Table S1) are in the range of 2.138(5)–2.146(5)

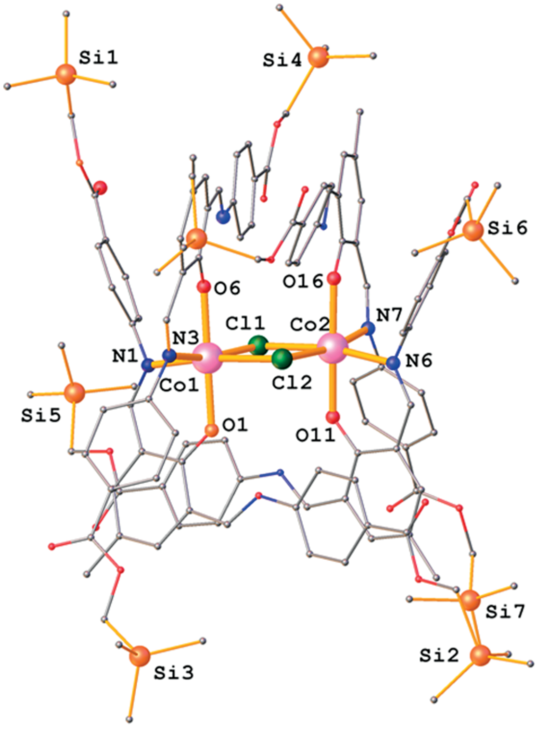

Figure 1. X-ray structure of the $[Co_2(\mu\text{-}Cl)_2(HL^2)_4]^{2+}$ dication in **1**.

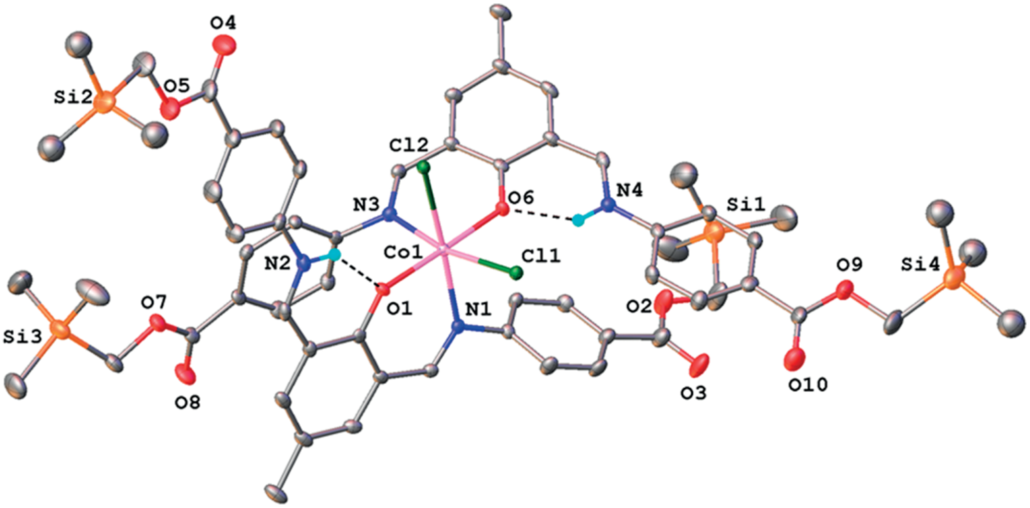

Figure 2. View of the coordination environment of the Co1 atom. H-bond parameters: N2–H···O1: N2–H 0.86 Å, H···O1 1.93 Å, N2···O1 2.609(6) Å, N2–H···O1 134.8°; N4–H···O6: N4–H 0.86 Å, H···O6 1.89 Å, N4···O6 2.582(6) Å, N4–H···O6 136.8°.

and 2.006(4)–2.039(4) Å, respectively. Two cobalt ions are linked by two μ-chlorido bridging ligands in *cis* positions to the nitrogen atoms of the Schiff base ligands, and the distance between the two cobalt atoms is 3.600(1) Å. The four Co–Cl bond lengths of the bridging μ-chlorido groups are between 2.462(2) and 2.518(2) Å, what is in a good agreement with those found for similar bis(μ-chlorido)Co^{II} complexes (2.359–2.628 Å).[26] Each Co atom displays a distorted $N_2O_2Cl_2$ octahedral *cis* geometry being coordinated by two zwitterionic HL^2 bidentate ligands and two bridging μ-chlorido atoms. The positional parameters of the protons attached to C=N groups were determined from a difference Fourier map, and their positional parameters were constrained accordingly. The perspective view of the Co1 site to show the coordination of the ligands is depicted in Figure 2. As can be seen, the noncoordinated imine nitrogen atoms from both HL^2 ligands act as proton donors in hydrogen bonding with the phenolato groups supporting the binding mode of the ligand. It should be noted that the Co_2Cl_2 coordination dinuclear core resembles well the similar one formed by Mn atoms in $[Mn_2Cl_2(H_2L)(HL)]Cl{\cdot}3H_2O$ and $[Mn_2Cl_2(H_2L)_2][MnCl_4]{\cdot}4CH_3CN{\cdot}0.5CHCl_3{\cdot}0.4H_2O$,[24] where H_2L is a product of the macrocyclic [2+2] condensation of DFF with 1,3-bis(3-aminopropyl)tetramethyldisiloxane.

Magnetic Properties

The temperature dependence of the magnetic susceptibility of **1** has been measured in the temperature range of 300–2 K in a magnetic field of 0.1 T, as shown in Figure 3. The value of $\chi_M T$ at 300 K is 9.749 $cm^3\,K\,mol^{-1}$, which is much larger than the expected spin-only value of 5.630 $cm^3\,K\,mol^{-1}$ for the three Co^{II} ions (S = 3/2) with g = 2.00 and suggests the presence of an important spin-orbital contribution characteristic to high-spin Co^{II}, as well as the ferromagnetic interaction. At temperatures of less than 50 K, the product $\chi_M T$ increases and reaches the maximal value of 11.208 $cm^3\,K\,mol^{-1}$ at 5 K. This implies the presence of the ferromagnetic interaction operating between two Co^{II} ions through two μ-chlorido bridges. The field dependence of magnetisation (Figure 3, inset) supports the presence of ferromagnetic interaction in **1**. The electron paramagnetic resonance (EPR) spectrum of a powdered sample of **1** is shown in Figure S4 and the recorded signals are in line with the interpretation obtained from magnetisation measurements.

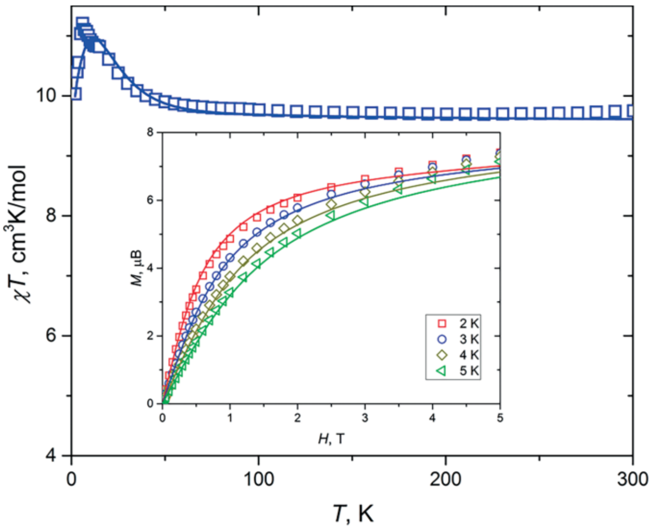

Figure 3. Experimental (symbols) and calculated (solid line) magnetic susceptibility data. Inset: calculated (solid lines) versus experimental (symbols) molar magnetisation curves of **1**.

Electronic and Magnetic Properties of Individual Cobalt Centers

Both CASSCF and CASPT2 calculations show that the ground state in the case of all cobalt ions corresponds to the spin S = 3/2 (Table S2). The calculated low-lying spin-orbital levels of the cobalt(II) centres are shown in Table 1. As can be seen, in the case of cobalt(II) ions, which are in an octahedral coordination environment, the ground Kramers doublets (KD) are well separated from the excited ones, while the cobalt(II) ion in the tetrahedral environment has a small zero-field splitting (ZFS). This implies that in the former case the spin-orbit coupling is operative in the first order of the perturbation theory and admixes strongly the low-lying spin-free states (Table S2). In the latter case, the spin-orbit coupling is operative only in the second order of the perturbation theory due to a larger energy gap between the ground and excited spin-free states (Table S2). As a result, a small ZFS is obtained (Table 1). Different environment of the cobalt ions has also influence on the *g*-factors of the ground KDs. For instance, transversal components of the **g**-tensor of Co1 and Co2 are smaller than the parallel component (Table 1), which means that in this case the magnetic anisotropy is of easy-axis type. On the other hand, in the case of Co3 transversal components of the **g**-tensor are larger than the parallel one, indicating an easy-plane type of anisotropy. Moreover, the angular momenta are also different: $<L_z>$ is large for Co1 and Co2 and small for Co3.

Table 1. Energies of the lowest Kramers doublets [cm^{-1}] of Co centres, *g*-factors and orbital moment (μ_B) of the ground KD obtained at the CASPT2 level.

Co1	Co2	Co3
0	0	0
209	188	13
649	703	2940
918	953	3100
1462	1483	
1507	1532	
$g_x = 1.71$	$g_x = 1.72$	$g_x = 5.12$
$g_y = 2.32$	$g_y = 2.29$	$g_y = 4.35$
$g_z = 7.96$	$g_z = 7.90$	$g_z = 2.27$
$<L_z> = 1.31$	$<L_z> = 1.27$	$<L_z> = 0.15$

Magnetic interaction between the nearest cobalt(II) centres was taken into account within the POLY_ANISO program, by employing the following Hamiltonian:

$$\hat{H} = -J^{exch}_{Co1-Co2}\hat{\mathbf{S}}_{Co1}\cdot\hat{\mathbf{S}}_{Co2}$$

where $S_{Co} = 3/2$. The exchange interaction with Co3 was set to zero, but its contribution to $\chi T(T)$ and $M(H)$ was taken into account explicitly.

The best fitting of the magnetic susceptibility data (Figure 3) is given by $J(Co_1–Co_2) = +8.8$ cm^{-1} and $zJ' = +0.006$ cm^{-1}, where zJ' accounts for the intermolecular interactions. Figure 3 (inset) shows that there is also a good agreement between the experimental and calculated magnetisation data. It is of note that the fitted exchange coupling parameter, $J(Co_1–Co_2) = +8.8$ cm^{-1}, matches well the one extracted from the BS-DFT calculations, $J(Co_1–Co_2) = +7.0$ cm^{-1}.

Electrochemistry

The redox properties of **1**, as well as those of the HL^2 and $[nBu_4N]_2[CoCl_4]$, for comparative purposes, have been investigated by cyclic voltammetry (CV) at a glassy carbon (GC) electrode in a 0.1 M $nBu_4N[BF_4]/CH_3CN$ solution at ambient temperature.

The cyclic voltammogram of the bis(μ-chlorido)-bridged dicobalt(II) complex **1** exhibits an irreversible reduction process (Figure 4a; I) at $E_p^{red} = –1.28$ V versus the Fc^+/Fc couple at a scan rate of 100 mV s^{-1}. Such reduction peak is absent in the CV of the HL^2 ligand (Figure 4b), as well as in that of the $[CoCl_4]^{2–}$ anion (Figure 4c). The comparison of the current intensity with Fc^+/Fc of the same concentration suggests a two-electron process. The peak can be tentatively assigned to the Co^{II}/Co^{I} reduction of both cobalt centres of the complex dication that occurs at similar reduction potentials. The absence of the reoxidation peak in the reverse scan indicates irreversible chemical changes of the dimeric dication upon reduction of the dicobalt core. The peak potential falls into the range reported for Co^{II}/Co^{I} reductions of related dinuclear Co complexes with amine–bis(phenolate) ligands,[10,27] complexes with similar Schiff bases[28] as well as cobaltoximes,[29] supporting the assignment performed. Further reduction at more negative potentials revealed additional irreversible reduction features with $E_p^{red} = –1.85$, –2.1 and –2.5 V, respectively (Figure 4a; II, III, IV). The current intensity points to the transfer of multiple electrons in the reduction processes involved. Comparison with the CVs of the proligand and the $[CoCl_4]^{2–}$ counterion indicates that the features in the range from –1.5 to –2.4 V likely represent an overlap of Co^{I}/Co^{0} reduction peaks of the transformed dicobalt cluster, and reduction of the ligand, while the peak at –2.5 V involves ligand reduction processes and the Co^{II}/Co^{I} reduction of the $[CoCl_4]^{2–}$ counterion. The anodic scan reveals an irreversible oxidation feature of multi-electron character in the CV of **1** with $E_p^{ox} = 1.14$ V (Figure 4a; V). It results from the superposition of peaks involving several oxidation processes, likely including the Co^{II}/Co^{III} oxidations {of the $[CoCl_4]^{2–}$[30] (Figure 4c) as well as both Co^{II} centres of the dimeric dication}, oxidation of the HL^2 (Figure 4b) and $Cl^–$ ligands in both $[CoCl_4]^{2–}$ and the dichlorido bridge.

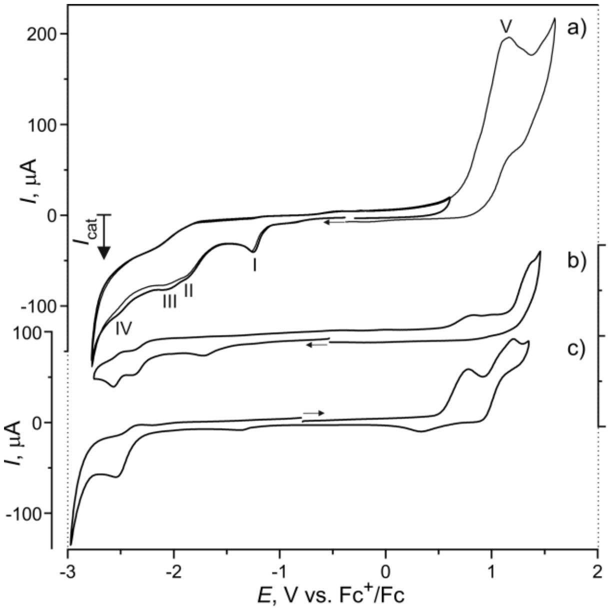

Figure 4. Cyclic voltammograms of (a) 1 mM **1**, (b) 1 mM HL^2 and (c) about 3 mM $[nBu_4N]_2[CoCl_4]$ in 0.1 M $nBu_4N[BF_4]/CH_3CN$ recorded by using a cylindrical GC working electrode at 100 mV s^{-1} at ambient temperature. Potential scan directions are indicated by an arrow. The CV peaks in (a) are labelled by roman numerals (see text).

Monomeric as well as dimeric Co complexes have been previously shown to act as efficient catalysts for the electrochemical H^+ reduction in the process of hydrogen production.[31] Cyclic voltammetry can be used as a quick test for catalytic activity estimation, since H_2 formation results in an increase of the catalytic current that is proportional to the concentration of H^+ and related to the TON of the catalysts. We have thus investigated the electrochemical response of **1** in the presence of increasing additions of trifluoroacetic acid (1–5 equiv.) as the proton donor. The presence of H^+ in the solution resulted in a progressive increase of the first reduction peak current and a minor shift of the peak potential from $E_p^{red} = -1.28$ V towards more positive values ($E_p^{red} = -1.26$ V with 5 equiv. of CF_3COOH) (Figure S5) that could indicate the H^+ reduction. However, additional new reduction and reoxidation peaks (some showing an adsorptive character) were found in the 0 to –1 V range indicating the interaction of the acid with the parent complex. This makes the interpretation of the voltammograms a complicated task. Moreover the only twofold increase in the peak current even in the presence of a fivefold excess of protons suggests a rather low TON and thus excludes **1** (and/or its follow-up products) as an efficient electrochemical H^+ reduction catalyst. However, the redox activity of **1** in the anodic part including multi-electron character indicates that this complex could be alternatively used in the catalytic oxidation of hydrocarbons as discussed in detail below.

Catalytic Studies

The catalytic activity of **1** was tested towards the homogeneous microwave (MW) assisted solvent-free oxidation of cyclohexane to cyclohexanol and cyclohexanone with aqueous *tert*-butyl hydroperoxide (*t*BuOOH, TBHP; see Scheme 2). The influence of varying catalyst amount, time and temperature as well as of adding an acid co-catalyst was evaluated (Table 2). No reaction

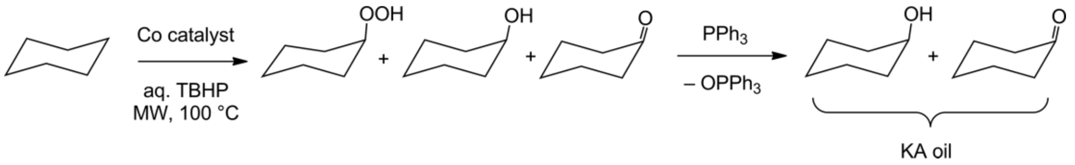

Scheme 2. Microwave-assisted neat oxidation of cyclohexane to cyclohexyl hydroperoxide, cyclohexanol and cyclohexanone with *tert*-butyl hydroperoxide catalysed by **1**.

Table 2. Selected data[a] for the MW-assisted oxidation of cyclohexane by *t*BuOOH (aq., 70 %) catalysed by $[Co_2(\mu\text{-}Cl)_2(HL^2)_4][CoCl_4]$.

Entry	Catalyst/substrate [%]	Co-catalyst [% vs. CyH]	Temperature [°C]	Reaction time [h]	Yield [%][b] CyO	CyOH	Total	TOF [h^{-1}][c]	Selectivity [%]
1	0.2	PCA	100	0.5	2.4	15.9	18.3	183	> 99
2		2.5		1.0	4.7	32.6	37.3	187	
3				1.5	20.9	31.9	52.8	176	
4[d]				1.5	24.8	18.4	43.2	144	
5				2.0	11.6	33.1	44.7	112	
6	0.2	–	100	0.5	0.0	12.5	12.5	125	> 99
7				1.0	9.9	18.3	28.2	141	
8				1.5	13.9	23.8	37.7	126	
9				2.0	13.2	17.4	30.6	77	
10	0.2	TEMPO	100	0.5	0.3	2.7	3.0	30	98
11		2.5		1.0	4.5	11.4	15.9	80	97
12				1.5	10.2	20.2	30.4	101	90
13				2.0	11.7	17.6	29.3	73	89
14	0.02	–	100	0.5	0.0	0.2	0.2	20	> 99
15				1.0	0.8	1.6	2.4	120	
16				1.5	1.8	5.2	7.0	233	
17				2.0	3.2	7.3	10.5	263	
18	0.2	–	60	0.5	0.0	0.3	0.3	3	98
19				1.0	3.1	4.1	7.2	36	99
20				1.5	5.2	11.2	16.4	55	96
21				2.0	6.9	16.1	23.0	56	96
22[e]	0.2	–	100	0.5	0.1	0.2	0.3	3	98
23[e]				1.0	1.2	1.7	2.9	15	
24[e]				1.5	1.6	1.8	4.4	11	
25[e]				2.0	3.6	5.7	9.3	23	

[a] Reaction conditions: cyclohexane (2.5 mmol), catalyst (0.5–5 μmol), *t*BuOOH (70 % in H_2O, 5 mmol), 60–100 °C. PCA = pyrazinecarboxylic acid. [b] mol of products [cyclohexanol (CyOH) + cyclohexanone (CyO)] per 100 mol of cyclohexane, as determined by GC after treatment with PPh_3. [c] TOF = mol of products per mol of catalyst per hour. [d] GC injection before treatment with PPh_3. [e] Oil-bath heating instead of MW irradiation.

was observed between cyclohexane and TBHP under MW irradiation at 100 °C for up to 3 h, while the presence of $CoCl_2{\cdot}6H_2O$ or $[CoCl_4]^{2-}$ salt led to a maximum total yield of 3 or 5.5 %, respectively, of oxygenated products. The best results were obtained when the reaction was performed at 100 °C for 1.5 h with use of a 0.2 % molar ratio of $[Co_2(\mu\text{-}Cl)_2(HL^2)_4][CoCl_4]$ relative to cyclohexane (Figure 5): cyclohexanol and cyclohexanone were formed in 53 % yield (Entry 3, Table 2; about ten times higher than those yields reported for the industrial aerobic process to assure a good selectivity).[32] No traces of by-products were detected by GC–MS analysis of the final reaction mixtures for the above optimised conditions.

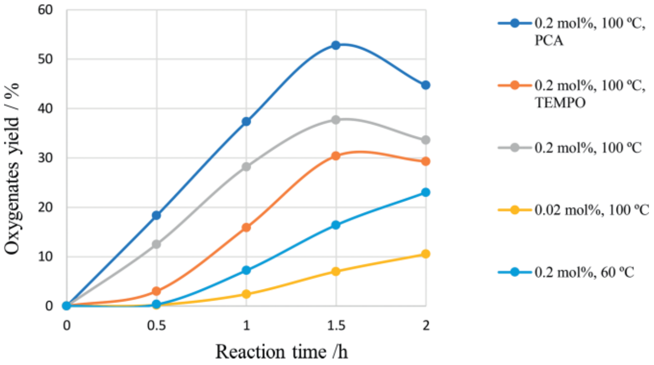

Figure 5. Effect of the reaction time, temperature, amount of $[Co_2(\mu\text{-}Cl)_2(HL^2)_4][CoCl_4]$ (0.02 or 0.2 mol-% catalyst/substrate ratio) and additives on the yield of KA oil obtained by microwave-assisted neat oxidation of cyclohexane with THBP.

The reaction is believed to proceed by a radical mechanism, through formation of cyclohexyl hydroperoxide (CyOOH), which further selectively leads to the KA oil [mixture of cyclohexanol (A) and cyclohexanone (K); Scheme 2] final product. In fact, by using Shul'pin's method,[33] the addition of PPh_3 prior to the GC analysis of the products, resulted in a marked increase (compare Entries 3 and 4, Table 2) of the amount of cyclohexanol due to the reduction of CyOOH to CyOH by PPh_3, with the formation of phosphane oxide (Scheme 2). Moreover, the suppression of the catalytic activity upon the introduction of the radical trap Ph_2NH to the reaction mixture also supports the hypothesis of a free-radical mechanism.[17–20,24,34]

The amount of catalyst, as well as the reaction temperature and time, have a significant influence on the catalytic activity of $[Co_2(\mu\text{-}Cl)_2(HL^2)_4][CoCl_4]$ as depicted in Figure 5.

The presence of PCA, although not essential for the catalytic activity of $[Co_2(\mu\text{-}Cl)_2(HL^2)_4][CoCl_4]$, enhances it significantly (Figure 5), allowing to reach 53 % yield of KA oil instead of 38 % obtained in the additive-free system (compare Entries 1–5 with 6–9, Table 2). On the other hand, TEMPO shows its usual[35] inhibiting effect (Figure 5 and Entries 1–5 and 10–13, Table 2) in radical catalytic systems.

Moreover, the used low-power MW-assisted reaction provides a much more efficient synthetic method of KA oil than conventional heating under open atmosphere or nonpressurised heating to reflux (Figure 6).

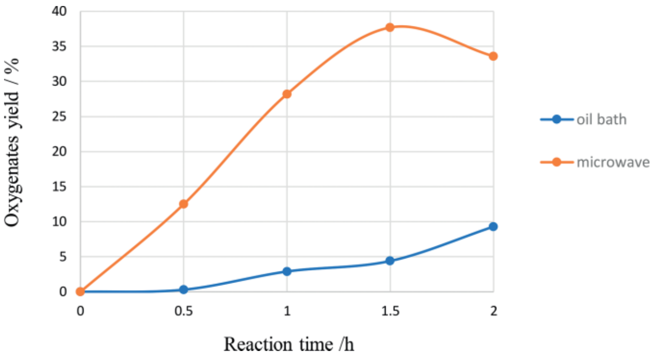

Figure 6. Effect of the heating mode on the yield of KA oil obtained by neat oxidation of cyclohexane with THBP.

Conclusions

In situ performed reaction of 2,6-diformyl-4-methylphenol with trimethylsilylmethyl *p*-aminobenzoate in a 1:2 molar ratio in a protic/aprotic solvent mixture, followed by addition of cobalt(II) chloride in the presence of a base resulted in the formation of a crude product, which after recrystallization afforded complex $[Co_2(\mu\text{-}Cl)_2(HL^2)_4][CoCl_4]{\cdot}4.5CH_3CN$ as confirmed by single-crystal X-ray diffraction analysis. Temperature dependence of magnetic susceptibility measurements and field dependence of magnetisation along with theoretical BS-DFT calculations indicate ferromagnetic interaction between the paramagnetic cobalt(II) (d^7, $S = 3/2$) centres in the dimeric dication and the presence of a different nature of spin-orbit coupling in the cation and $[CoCl_4]^{2-}$. The electrochemical response of **1** in the presence of increasing amounts of CF_3COOH (1–5 equiv.) resulted in a progressive increase of the first reduction peak current that could indicate the H^+ reduction. The relatively low increase of the first reduction peak and the presence of new reduction and reoxidation peaks, implying the interaction of the acid with the parent complex, and overall its low stability in solution made further investigation of the electrochemical reduction useless. However, complex **1** acts as a homogeneous precatalyst in the MW-assisted neat oxidation of cyclohexane with TBHP (aq.), through a radical mechanism, affording KA oil in high selectivity and in a yield that is about ten times higher than that of the current industrial process. Other advantages of the present catalytic systems are the mild and environmentally benign conditions such as (i) solvent-free protocol, (ii) use of environmentally acceptable oxidant [TBHP (aq.)] and energy source (MW irradiation), and (iii) short reaction time. These are significant features towards the development of a sustainable chemical process for the cyclohexane oxidation to KA oil.

Experimental Section

Materials: Trimethylsilylmethyl *p*-aminobenzoate was prepared from (chloromethyl)trimethylsilane (Aldrich) and *p*-aminobenzoic acid sodium salt by applying a published procedure.[25] 2,6-Diformyl-4-methylphenol (Polivalent-95), $CoCl_2{\cdot}6H_2O$ (Aldrich), triethylamine, diphenylamine, cyclohexane (Fluka), methanol, chloroform (Chimopar), acetonitrile, *tert*-butyl hydroperoxide [TBHP (aq.), 70 %], nitromethane, triphenylphosphane (Aldrich), acetonitrile (CH_3CN; Aldrich) and trifluoroacetic acid (CF_3COOH) were received from commercial sources and used without further purification. Tetrabutylammonium tetrafluoroborate ($n\mathrm{Bu}_4\mathrm{N}[\mathrm{BF}_4]$; 99 %, Sigma–Aldrich) was dried under reduced pressure at 70 °C for 24 h and stored in a desiccator before use. Ferrocene (98 %, Sigma–Aldrich) was employed as internal potential standard in electrochemical measurements. $[n\mathrm{Bu}_4\mathrm{N}]_2[\mathrm{CoCl}_4]$ was prepared from $n\mathrm{Bu}_4\mathrm{NCl}$ (Aldrich) and CoCl_2 (Mikrochem) (2:1 molar ratio) in a small volume of absolute ethanol as described previously.[36]

$[\mathrm{Co}_2(\mu\text{-Cl})_2(\mathrm{HL}^2)_4][\mathrm{CoCl}_4]\cdot 4.5\mathrm{CH}_3\mathrm{CN}$: To a solution of 2,6-diformyl-4-methylphenol (0.164 g, 1.0 mmol) in a methanol/chloroform mixture (1:1, v/v; 10 mL) was added a solution of trimethylsilylmethyl *p*-aminobenzoate (0.446 g, 2.0 mmol) in methanol/chloroform (1:1, v/v; 10 mL). The reaction mixture was stirred at reflux for 3 h. A solution of $\mathrm{CoCl}_2\cdot 6\mathrm{H}_2\mathrm{O}$ (0.476 g, 2 mmol) in methanol/chloroform (1:1, v/v; 10 mL) was slowly added to the reaction mixture and stirred at 50 °C for 30 min. The colour changed from orange to dark red. Then, a few drops of triethylamine were added, and the reaction mixture was stirred at 50 °C for 10 min. The resulting solution was cooled to room temperature and left to stand for crystallisation. The obtained red-brown precipitate was recrystallised from a chloroform/acetonitrile mixture (1:1, v/v; 10 mL) to give red-brown crystals, which were collected by filtration, washed with cold chloroform/acetonitrile (1:1; 3 × 5 mL) and dried in air. Yield: 27.0 % (196 mg). $\mathrm{C}_{133}\mathrm{H}_{162.5}\mathrm{Cl}_6\mathrm{Co}_3\mathrm{N}_{12.5}\mathrm{O}_{20}\mathrm{Si}_8$ (2870.52): calcd. C 55.65, H 5.71, N 6.10; found C 55.23, H 5.30, N 5.77. HRMS (ESI+, acetonitrile): m/z = 1272.3258 $[\mathrm{Co}_2\mathrm{Cl}_3(\mathrm{L}^2)_2(\mathrm{HL}^2)_2]^{2+}$. IR (KBr): $\tilde{\nu}_{\max}$ = 3425 (m), 3057 (vw), 2955 (m), 2904 (w), 1714 (vs), 1636 (vs), 1622 (w), 1599 (s), 1537 (vs), 1501 (m), 1414 (w), 1388, 1313 (vs), 1303 (vs), 1249 (vs), 1237 (s), 1198 (s), 1172 (s), 1110 (s), 1071 (m), 1015 (m), 1000 (m), 854 (vs), 766 (s), 732 (w), 701 (m), 622 (vw), 602 (vw), 519 (w), 395 (w) cm^{-1}. UV/Vis (acetonitrile): $\lambda_{\max}$ (ε) = 262 (23480), 314 (18330), 470 (8315), 585 (339), 631 (173), 660 (256), 685 (288 $\mathrm{M}^{-1}\,\mathrm{cm}^{-1}$) nm.

Analytical and Spectroscopic Measurements: Infrared (IR) spectra were recorded with a Bruker Vertex 70 FTIR spectrometer. Registrations were performed in transmission mode within a 400–4000 cm^{-1} range at room temperature with a resolution of 4 cm^{-1} and accumulation of 32 scans. Elemental (C, H, N) analyses were obtained with a Perkin–Elmer CHNS 2400 II elemental analyser. High-resolution electrospray ionisation mass spectra [HRMS (ESI)] were recorded with a maXis instrument by using acetonitrile as a solvent. A UV/Vis absorption spectrum of the complex in acetonitrile was measured with a Specord 200 spectrophotometer.

Magnetic Measurements: Magnetic susceptibility data (2–300 K) were collected on powdered polycrystalline samples by a SQUID magnetometer with a Quantum Design model MPMS instrument and under an applied magnetic field of 0.1 T. The magnetisation isotherm was recorded at 2 K between 0 and 5 T. All data were corrected for the contribution of the sample holder and diamagnetism of the samples estimated by using Pascal's constants.[37,38]

X-ray Crystallography: Crystallographic measurements for **1** were carried out with an Oxford Diffraction XCALIBUR E CCD diffractometer equipped with graphite-monochromated Mo-K_α radiation. The single crystal was positioned at 40 mm from the detector, and 140 frames were measured, each over 1° scan width for 30 s. The unit-cell determination and data integration were performed by using the CrysAlis package of Oxford Diffraction.[39] The structure was solved by direct methods with use of Olex2[40] software with the SHELXTL structure solution program and refined by full-matrix least squares on F^2 with SHELXL-97[41] by using an anisotropic model for non-hydrogen atoms. H atoms were placed at calculated positions and refined as riding atoms in the subsequent least-squares model refinements. The positional parameters of NH hydrogen atoms were obtained from difference Fourier syntheses and verified by the geometric parameters of the corresponding hydrogen bonds. The positional parameters of the disordered moieties were refined in combination with PART and SADI restrains by using an anisotropic/isotropic model for non-H atoms. The molecular plots were obtained by using the Olex2 program. Table 3 provides a summary of the crystallographic data together with refinement details for **1**. CCDC 1561444 (for **1**) contains the supplementary crystallographic data for this paper. These data can be obtained free of charge from The Cambridge Crystallographic Data Centre.

Table 3. Crystallographic data, details of data collection and structure refinement parameters for **1**.

Empirical formula	$\mathrm{C}_{133}\mathrm{H}_{162.5}\mathrm{Cl}_6\mathrm{Co}_3\mathrm{N}_{12.5}\mathrm{O}_{20}\mathrm{Si}_8$
Formula mass [g mol^{-1}]	2870.47
Temperature [K]	173
Crystal system	monoclinic
Space group	$P2_1/n$
a [Å]	22.3644(8)
b [Å]	32.0968(7)
c [Å]	23.2738(8)
β [°]	111.132(4)
V [Å^3]	15583.1(9)
Z	4
$D_{\mathrm{calcd.}}$ [mg mm^{-3}]	1.224
μ [mm^{-1}]	0.542
Crystal size [mm]	0.40 × 0.35 × 0.35
$\theta_{\min}$, $\theta_{\max}$ [°]	3.16, 46.52
Reflections collected	55816
Independent reflections (R_{int} = 0.0542)	22342
Data/restraints/parameters	22342/89/1622
R_1[a] [$I > 2\sigma(I)$]	0.0792
wR_2[b] (all data)	0.2293
GOF[c]	1.029
Largest diff. peak/hole [e Å^{-3}]	2.50/–2.50

[a] $R_1 = \Sigma||F_o| - |F_c||/\Sigma|F_o|$. [b] $wR_2 = \{\Sigma[w(F_o^2 - F_c^2)^2]/\Sigma[w(F_o^2)^2]\}^{1/2}$. [c] GOF = $\{\Sigma[w(F_o^2 - F_c^2)^2]/(n - p)\}^{1/2}$, where n is the number of reflections and p is the total number of parameters refined.

Electrochemistry: Cyclic voltammograms were recorded in $\mathrm{CH}_3\mathrm{CN}$ with $n\mathrm{Bu}_4\mathrm{N}[\mathrm{BF}_4]$ (0.1 M) as the supporting electrolyte by using a one-compartment electrochemical cell with a glassy carbon (GC) cylindrical working electrode, Pt coil as counter electrode, and Ag wire pseudoreference electrode. All electrochemical measurements were performed under argon by using the HEKA PG 390 potentiostat. The $\mathrm{Fc}^+/\mathrm{Fc}$ couple served as an internal standard.

Computational Details: All calculations were carried out with MOLCAS 8.0 program[42] and are of CASSCF/CASPT2/SO-RASSI/SINGLE_ANISO type. Structures of the calculated Co fragments are shown in Figure S6. Each magnetic centre was calculated by replacing the neighbouring $\mathrm{Co}^{\mathrm{II}}$ ion by a nonmagnetic $\mathrm{Zn}^{\mathrm{II}}$ ion. Information about the employed basis set is given in Table S3. Active space of the CASSCF method[43] included 7 electrons in 10 orbitals (3d and 3d′ orbitals of Co^{2+} ion) to account for the double-shell effect.[44] The dynamical electron correlation energy was considered within CASPT2 calculations.[45] The imaginary shift was set to 0.1. All obtained quartet (10) and doublet states (40) were mixed by spin-orbit coupling within SO-RASSI program.[46] On the basis of the resulting spin-orbital multiplets the SINGLE_ANISO program[47] computed local magnetic properties. The exchange interaction was accounted within the Lines model[48] by employing POLY_ANISO program[49] and by using the results obtained from the CASPT2 calculations. Broken-symmetry DFT calculations have been carried out to estimate the value of the exchange coupling constant between the closest (octahedral) Co centres, by using the structure shown in Figure S7. The SVP basis set and the B3LYP functional were used as implemented in the ORCA 3.0.0 program.[50] Scalar relativistic effects were included within the Douglas–Kroll–Hess Hamiltonian. The exchange coupling constant was calculated by using Yamaguchi's formula.[51]

Catalytic Studies: The catalytic oxidations of cyclohexane were performed in sealed cylindrical (5 mL capacity with a 1 cm internal diameter) Pyrex tubes, under focused microwave irradiation (MW), in an Anton Paar Monowave 300 reactor fitted with a rotational system and an IR temperature detector. Typical reaction conditions are as follows: a tube was charged with (in this order) cyclohexane (2.50 mmol), catalyst (0.5–5 µmol) and *tert*-butyl hydroperoxide (TBHP) (aq., 70 %, 5.00 mmol). For the assays in the presence of a radical trap, $NHPh_2$ in stoichiometric amount relative to the oxidant was added to the reaction mixture. The tube was placed in the microwave reactor and the mixture was stirred (600 rpm) and irradiated (10 W) at 60 or 100 °C for 0.5–24 h. After the reaction, the mixture was allowed to cool to room temperature. Solution samples were analysed by gas chromatography (GC) after addition of nitromethane (as the internal standard compound). For reactions performed under conventional heating, round-bottomed flasks (5 mL) equipped with reflux condensers in conventional oil baths in air were used. The reagents (see above) were added to the flask and vigorously stirred at the desired temperature (60–100 °C) for the desired reaction time (up to 24 h). The products were analysed as described above. GC analyses were carried out by using a FISONS Instruments GC 8000 series gas chromatograph with a FID detector and a capillary column (DB-WAX, column length: 30 m; internal diameter: 0.32 mm) and the Jasco–Borwin v.1.50 software. The temperature of injection was 240 °C. The initial temperature was maintained at 100 °C for 1 min, then raised 10 °C/min to 160 °C and maintained at this temperature for 1 min. Helium was used as the carrier gas. GC–MS analyses were performed by using a Perkin–Elmer Clarus 600 C instrument (He as the carrier gas). The ionisation voltage was 70 eV. Gas chromatography was conducted in the temperature-programming mode, by using an SGE BPX5 column (30 m × 0.25 mm × 0.25 µm). Considering that the reaction mixture contains cyclohexyl hydroperoxide (primary product), cyclohexanol and cyclohexanone, an excess of solid triphenylphosphane was added (to reduce the cyclohexyl hydroperoxide to the corresponding alcohol, and hydrogen peroxide to water), and the mixture was analysed again to estimate the amount of cyclohexyl hydroperoxide, according to a method developed by Shul'pin.[33] For precise determination of the product concentrations only data obtained after the reduction of the reaction sample with triphenylphosphane were typically used. Reaction products were identified by comparison of their retention times with those of known reference compounds, and by comparing their mass spectra to fragmentation patterns obtained from the NIST spectral library stored in the computer software of the mass spectrometer. Blank experiments, in the absence of any catalyst, were performed under the studied reaction conditions, and no significant conversion was observed.

Acknowledgments

We would like to thank Liviu Chibotaru for useful discussions. Financial support from the Fundação para a Ciência e a Tecnologia (FCT), Portugal, for the CATSUS fellowship (SFRH/BD/52371/2013) to N. M. R. M. and the PTDC/QEQ-ERQ/1648/2014, PTDC/QEQ-QIN/3967/2014 and UID/QUI/00100/2013 projects, is gratefully acknowledged. V. V. acknowledges the postdoctoral fellowship of the Fonds Wetenschappelijk Onderzoek-Vlaanderen (FWO, Flemish Science Foundation). This work was also supported by the Science and Technology Assistance Agency under contract no. APVV-15-0053 and by the Slovak Grant Agency VEGA under contract no. 1/0416/17 and a grant of the Ministry of Research and Innovation, CNCS – UEFISCDI [project number PN-III-P4-ID-PCE-2016-0642 within PNCDI III (contract 114/2017)].

Keywords: Cobalt · Silicon · Schiff bases · Catalyst precursors · Oxidation · Cyclohexane

[1] J. Sun, J. P. Bigi, N. A. Piro, M. L. Tang, J. R. Long, C. J. Chang, *J. Am. Chem. Soc.* **2011**, *133*, 9212–9215.
[2] B. Das, A. Orthaber, S. Ott, A. Thapper, *Chem. Commun.* **2015**, *51*, 13074–13077.
[3] C. C. L. McCrory, C. Uyeda, J. C. Peters, *J. Am. Chem. Soc.* **2012**, *134*, 3164–3170.
[4] L. Tong, R. Zong, R. P. Thummel, *J. Am. Chem. Soc.* **2014**, *136*, 4881–4884.
[5] W. M. Singh, T. Baine, S. Kudo, S. Tian, X. A. N. Ma, H. Zhou, N. Y. DeYonker, T. C. Pham, J. C. Bollinger, G. L. Baker, B. Yan, C. E. Webster, X. Zhao, *Angew. Chem. Int. Ed.* **2012**, *51*, 5941–5944; *Angew. Chem.* **2012**, *124*, 6043.
[6] F. Lakadamyali, M. Kato, N. M. Muresan, E. Reisner, *Angew. Chem. Int. Ed.* **2012**, *51*, 9381–9384; *Angew. Chem.* **2012**, *124*, 9515–9518.
[7] Y. Zhao, J. Lin, Y. Liu, B. Ma, Y. Ding, M. Chen, *Chem. Commun.* **2015**, *51*, 17309–17312.
[8] H. Chen, Z. Sun, X. Liu, A. Han, P. Du, *J. Phys. Chem. C* **2015**, *119*, 8998–9004.
[9] L.-Z. Fu, L.-L. Zhou, S.-Z. Zhan, *RSC Adv.* **2015**, *5*, 84770–84775.
[10] Y.-X. Zhang, L.-Z. Fu, L.-L. Zhou, S.-Z. Zhan, W. Li, *Synth. Met.* **2016**, *212*, 69–74.
[11] L.-Z. Fu, L.-L. Zhou, Q.-N. Liang, C. Fang, S.-Z. Zhan, *Polyhedron* **2016**, *107*, 83–88.
[12] H.-Y. Wang, E. Mijangos, S. Ott, A. Thapper, *Angew. Chem. Int. Ed.* **2014**, *53*, 14499–14502; *Angew. Chem.* **2014**, *126*, 14727.
[13] M. Chen, S.-M. Ng, S.-M. Yiu, K.-C. Lau, R. J. Zeng, T. C. Lau, *Chem. Commun.* **2014**, *50*, 14956–14959.
[14] S. Ribeiro, L. Cunha-Silva, S. S. Balula, S. Gago, *New J. Chem.* **2014**, *38*, 2500–2507.
[15] A. Panja, P. Guionneau, *Dalton Trans.* **2013**, *42*, 5068–5075.
[16] P. Yu, S. Gao, R. Tang, *Curr. Organocat.* **2015**, *2*, 203–211.
[17] T. F. S. Silva, L. M. D. R. S. Martins, M. F. C. Guedes da Silva, M. L. Kuznetsov, A. R. Fernandes, A. Silva, C.-J. Pan, J.-F. Lee, B.-J. Hwang, A. J. L. Pombeiro, *Chem. Asian J.* **2014**, *9*, 1132–1143.
[18] T. F. S. Silva, K. V. Luzyanin, M. V. Kirillova, M. F. C. Guedes da Silva, L. M. D. R. S. Martins, A. J. L. Pombeiro, *Adv. Synth. Catal.* **2010**, *352*, 171–187.
[19] T. F. S. Silva, G. S. Mishra, M. F. C. Guedes da Silva, R. Wanke, L. M. D. R. S. Martins, A. J. L. Pombeiro, *Dalton Trans.* **2009**, 9207–9215.
[20] T. F. S. Silva, E. C. B. A. Alegria, L. M. D. R. S. Martins, A. J. L. Pombeiro, *Adv. Synth. Catal.* **2008**, *350*, 706–716.
[21] A. Soroceanu, M. Cazacu, S. Shova, C. Turta, J. Kožišek, M. Gall, M. Breza, P. Rapta, T. C. O. Mac Leod, A. J. L. Pombeiro, J. Telser, A. A. Dobrov, V. B. Arion, *Eur. J. Inorg. Chem.* **2013**, 1458–1474.
[22] M. Cazacu, S. Shova, A. Soroceanu, P. Machata, L. Bucinsky, M. Breza, P. Rapta, J. Telser, J. Krzystek, V. B. Arion, *Inorg. Chem.* **2015**, *54*, 5691–5706.
[23] A. Vlad, C. Turta, M. Cazacu, E. Rusu, S. Shova, *Eur. J. Inorg. Chem.* **2012**, 5078–5084.
[24] M. Alexandru, M. Cazacu, A. Arvinte, S. Shova, C. Turta, B. C. Simionescu, A. Dobrov, E. B. C. A. Alegria, L. M. D. R. S. Martins, A. J. L. Pombeiro, V. B. Arion, *Eur. J. Inorg. Chem.* **2014**, 120–131.
[25] M.-F. Zaltariov, M. Alexandru, M. Cazacu, S. Shova, G. Novitchi, C. Train, A. Dobrov, M. V. Kirillova, E. C. B. A. Alegria, A. J. L. Pombeiro, V. B. Arion, *Eur. J. Inorg. Chem.* **2014**, 4946–4956.
[26] S. G. Telfer, T. Sato, R. Kuroda, J. Lefebvre, D. B. Leznoff, *Inorg. Chem.* **2004**, *43*, 421–429.

[27] a) T. C. Davenport, T. D. Tilley, *Dalton Trans.* **2015**, *44*, 12244–12255; b) P. Ghosh, S. Samanta, S. K. Roy, S. Joy, T. Krämer, J. E. McGrady, S. Goswami, *Inorg. Chem.* **2013**, *52*, 14040–14049.

[28] J. E. Armstrong, P. M. Crossland, M. A. Frank, M. J. Van Dongen, W. R. McNamara, *Dalton Trans.* **2016**, *45*, 5430–5433.

[29] a) P.-A. Jacques, V. Artero, J. Pécaut, M. Fontecave, *Proc. Natl. Acad. Sci. USA* **2009**, *106*, 20627–20632; b) M. A. W. Lawrence, M. J. Celestine, E. T. Artis, L. S. Joseph, D. L. Esquivel, A. J. Ledbetter, D. M. Cropek, W. L. Jarrett, C. A. Bayse, M. I. Brewer, A. A. Holder, *Dalton Trans.* **2016**, *45*, 10326–10342.

[30] C. Moyses Araujo, M. D. Doherty, S. J. Konezny, O. R. Luca, A. Usyatinsky, H. Grade, E. Lobkovsky, G. L. Soloveichik, R. H. Crabtree, V. S. Batista, *Dalton Trans.* **2012**, *41*, 3562–3573.

[31] a) V. Artero, M. Chavarot-Kerlidou, M. Fontecave, *Angew. Chem. Int. Ed.* **2011**, *50*, 7238–7266; *Angew. Chem.* **2011**, *123*, 7376; b) N. Kaeffer, M. Chavarot-Kerlidou, V. Artero, *Acc. Chem. Res.* **2015**, *48*, 1286–1295; c) N. K. Szymczak, L. A. Berben, J. C. Peters, *Chem. Commun.* **2009**, 6729–6731.

[32] *Ullmann's Encyclopedia of Industrial Chemistry*, 6th ed., Wiley-VCH, Weinheim, **2002**.

[33] a) G. B. Shul'pin, *Transition Metals for Organic Synthesis* (Eds.: M. Beller, C. Bolm), 2nd ed., Wiley-VCH, New York, **2004**, vol. 2, p. 215; b) G. B. Shul'pin, G. V. Nizova, *React. Kinet. Catal. Lett.* **1992**, *48*, 333–338; c) G. B. Shul'pin, M. G. Matthes, V. B. Romakh, M. I. F. Barbosa, J. L. T. Aoyagi, D. Mandelli, *Tetrahedron* **2008**, *64*, 2143–2152; d) G. B. Shul'pin, *Dalton Trans.* **2013**, *42*, 12794–12818; e) G. B. Shul'pin, *Org. Biomol. Chem.* **2010**, *8*, 4217–4228; f) G. B. Shul'pin, *Mini-Rev. Org. Chem.* **2009**, *6*, 95–104.

[34] A. J. L. Pombeiro (Ed.), *Advances in Organometallic Chemistry and Catalysis, The Silver/Gold Jubilee ICOMC Celebratory Book*, John Wiley & Sons, Hoboken, New Jersey, **2014**.

[35] a) G. Strukul, A. Scarso, “Environmentally Benign Oxidants” in *Liquid Phase Oxidation via Heterogeneous Catalysis, Organic Synthesis and Industrial Applications* (Eds.: M. G. Clerici, O. Kholdeeva), John Wiley & Sons, New Jersey, **2013**, chapter 1; b) L. M. Slaughter, J. P. Collman, T. A. Eberspacher, J. I. Brauman, *Inorg. Chem.* **2004**, *43*, 5198–5204.

[36] a) L. A. Kushch, E. B. Yagubskii, S. V. Simonov, R. P. Shibaeva, E. A. Suturina, N. P. Gritsan, A. V. Sadakov, I. V. Sulimenkov, *Eur. J. Inorg. Chem.* **2013**, 5603–5611; b) F. A. Cotton, D. M. L. Goodgame, M. Goodgame, *J. Am. Chem. Soc.* **1961**, *83*, 4690–4699.

[37] G. A. Bain, J. F. Berry, *J. Chem. Educ.* **2008**, *85*, 532–536.

[38] O. Kahn, *Molecular Magnetism*, VCH Publishers, New York, Weinheim, Cambridge, **1993**.

[39] *CrysAlis RED*, version 1.171.36.32, Oxford Diffraction Ltd., **2003**.

[40] O. V. Dolomanov, L. J. Bourhis, R. J. Gildea, J. A. K. Howard, H. Puschmann, *J. Appl. Crystallogr.* **2009**, *42*, 339–341.

[41] G. M. Sheldrick, *Acta Crystallogr., Sect. A* **2008**, *64*, 112–122.

[42] F. Aquilante, J. Autschbach, R. K. Carlson, L. F. Chibotaru, M. G. Delcey, L. De Vico, I. F. Galvan, N. Ferré, L. M. Frutos, L. Gagliardi, M. Garavelli, A. Giussani, C. E. Hoyer, G. L. Manni, H. Lischka, D. Ma, P. Å. Malmqvist, T. Müller, A. Nenov, M. Olivucci, T. B. Pedersen, D. Peng, F. Plasser, B. Pritchard, M. Reiher, I. Rivalta, I. Shapiro, J. Segarra-Martí, M. Stenrup, D. G. Truhlar, L. Ungur, A. Valentini, S. Vancoillie, V. Veryazov, V. P. Vysotskiy, O. Weingart, F. Zapata, R. Lindh, *J. Comput. Chem.* **2016**, *37*, 506–541.

[43] B. O. Roos, P. R. Taylor, P. E. M. Siegbahn, *Chem. Phys.* **1980**, *48*, 157–173.

[44] K. Andersson, B. O. Roos, *Chem. Phys. Lett.* **1992**, *191*, 507–514.

[45] K. Andersson, P.-Å. Malmqvist, B. O. Roos, *J. Chem. Phys.* **1992**, *96*, 1218.

[46] P.-Å. Malmqvist, B. O. Roos, *Chem. Phys. Lett.* **1989**, *155*, 189–194.

[47] a) L. F. Chibotaru, L. Ungur, *Chem. Phys.* **2012**, *137*, 064112; b) http://molcas.org/documentation/manual/.

[48] M. E. Lines, *J. Chem. Phys.* **1971**, *55*, 2977.

[49] L. F. Chibotaru, L. Ungur, C. Aronica, H. Elmoll, G. Pilet, D. Luneau, *J. Am. Chem. Soc.* **2008**, *130*, 12445–12455.

[50] F. Neese, *WIREs Comput. Mol. Sci.* **2012**, *2*, 73–78.

[51] T. Soda, Y. Kitagawa, T. Onishi, Y. Takano, Y. Shigeta, H. Nagao, Y. Yoshioka, K. Yamaguchi, *Chem. Phys. Lett.* **2000**, *319*, 223–230.

Received: July 19, 2017